Airport Pavement Roughness with Nighttime Construction

Gordon F. Hayhoe
Federal Aviation Administration, William J. Hughes Technical Center, AAR-410
USA

Mingyao Dong
Galaxy Scientific Corporation, Egg Harbor Township, NJ
USA

Roy D. McQueen
Roy D. McQueen & Associates, Ltd., Oakton, VA
USA

ABSTRACT

Surface elevation profiles were measured before and after overlay operations on runways at two commercial airports in the USA. Each airport had only one runway. All overlaying was done at night, with the airports opened for normal operations during the day. The profiles were measured with an inertial profiler having software compensation for accelerometer errors. Pavement surface elevations measured with normal surveying rod and level equipment are compared with the profiler elevation measurements for one of the runways. With the exception of some very long wavelength distortion in the profiler measurements, correspondence between the two different methods is good. The profiles were processed to provide measures of roughness from simulations of a straightedge, a California Profilograph, and the Boeing Bump Criteria. The roughness of the overlaid pavements is quantified and compared. Measurements of the vertical response of an instrumented B-727 aircraft on one of the runways are also presented. Transverse construction joints are shown to be significant contributors to the roughness of the pavements.

INTRODUCTION

Pavement maintenance and rehabilitation at commercial airports has to be performed with minimum disruption of aircraft service. For large international airports, and for airports with only one runway, this almost always means that major pavement work, such as overlaying and rehabilitation, must be done at night in a series of short "pulls." The pressure of rapid work, combined with frequent lateral construction joints, can lead to runways which are not as smooth as can be achieved when the runway is completely shut down and the work is done continuously. In order to make a determination of the levels of roughness which are achieved during intermittent construction, two runway overlay rehabilitation projects were selected for study.

The first (referred to here as R1) was a flexible pavement which was structurally sound but had suffered surface deterioration due, primarily, to cracking and weathering. To restore the surface, a nominal 75-mm (3-inch) overlay was applied to controlled grade. The second (R2) was a very old rigid pavement which had been lightly overlaid to seal the surface until the runway could be rehabilitated. Rehabilitation consisted of a crack-and-seat operation followed by application of a nominal 200-mm (8-inch) thick overlay. Construction was phased, with 625-m (2,000-ft) sections at each end of the runway constructed during the daytime using displaced thresholds. The 2,500-m (8,000-ft) center section of the runway was then re-constructed at night in a series of 7-hour closures. During the nighttime operations on both of the runways, the overlays were placed over the full width in a single night in pull lengths of 100 to 150 m (300 to 450 ft).

Elevation profiles of the two runways were measured before and after the construction operations using an inertial profiler. The profiler was developed under FAA funding specifically for rapid

measurement of elevation profiles on airport runways and taxiways. The equipment is portable so that it can be easily transported as aircraft baggage. Distance to the pavement surface is measured with a small spot-size laser sensor at a very high data rate so that lateral grooving can be measured and, where necessary, correctly filtered out of the profile. Vertical (inertial) position of the test vehicle is found by open loop integration of the vertical accelerometer signal. Stabilizing compensation is applied in the data processing software using a least-squares minimization scheme. Errors in the vertical accelerometer signal due to acceleration and braking of the test vehicle are also compensated for as part of the minimization scheme. Use of the compensation eliminates the need to stabilize the integration process by high-pass filtering, as is normally done with highway profile measurements (Pong, 1991). Distortion of the profile over long disturbances is therefore reduced and it is easier to visually identify specific disturbances in the measured profile. Rod and level survey measurements made prior to overlaying runway R1 were also obtained from the construction contractor.

Roughness indices were computed from the measured profiles to evaluate the change in roughness from before to after the paving operations, and to make a determination of the levels of roughness which were achieved during the operations. Indices computed were 3.7 m (12-ft) straightedge, California Profilograph, and an adaptation of the Boeing Bump Criteria (DeBord, 1992).

PROFILE MEASUREMENT

A typical inertial profiler consists of three major components: a sensor to measure the distance from a point on the test vehicle to the pavement surface; an accelerometer to measure the vertical acceleration of the test vehicle; and a sensor for measuring the distance traveled along the pavement.

The profiler that was used has a laser triangulation-type distance measuring sensor with a nominal spot size of 1 mm (0.04 in), a measurement range of ± 100 mm (4 in), a resolution of 12-bits (0.049 mm, 0.002 in), and a sample rate of 32 kHz. The normal test speed is 60 km/h and the maximum spatial sampling distance is therefore 0.52 mm/sample (0.02 in/sample), or one-half the spot size per sample. (There will also be more than 10 samples taken while traversing a 6-mm groove.)

A high quality servo accelerometer measures the vertical acceleration of the test vehicle and a non-contact incandescent light distance sensor measures traveled distance (output is one pulse every 2.5 mm (0.1 in)). Inertial profiling devices were originally developed for highway use and measurements with these devices are typically made at a constant travel speed. However, runways and taxiways normally have closed ends and, in order to measure the profile along the full length of a runway or taxiway, measurements must be made while the test vehicle is accelerating or braking. This can introduce extremely large errors into the profile measurement. (High-pass filtering the profile will not remove the errors unless a very short cutoff wavelength is used.)

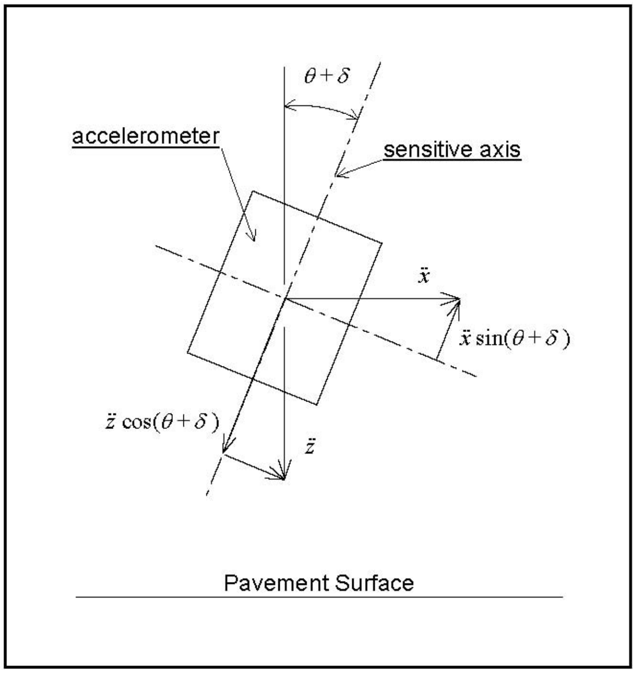

Figure 1 illustrates how the errors arise. The sensitive axis of the accelerometer is usually inclined at some small angle *(*θ*)* to the desired measurement axis (which is perpendicular to the pavement surface). In addition, a change of inclination angle *(*δ*)* also occurs whenever the test vehicle pitches under acceleration or braking. Because of the inclination of the accelerometer to the pavement surface, a component of the longitudinal acceleration of the test vehicle is coupled into the sensitive axis of the accelerometer, causing significant errors if the vehicle accelerates or brakes. Using the nomenclature:

Figure 1. Acceleration coupling errors.

θ = initial accelerometer angle offset perpendicular to the pavement surface.
δ = vehicle pitch angle from initial offset position.
$\ddot{z}$ = vehicle acceleration perpendicular to the pavement surface (bounce).
$\ddot{x}$ = vehicle acceleration parallel to the pavement surface (acceleration and braking).
$\ddot{z}\cos(\theta+\delta)$ = component of vertical acceleration along the sensitive axis.
$\ddot{x}\sin(\theta+\delta)$ = component of longitudinal acceleration along the sensitive axis.

The acceleration measured by the accelerometer along its sensitive axis can be written as:

$$\ddot{z}_M = \ddot{z}\cos(\theta+\delta) - \ddot{x}\sin(\theta+\delta)$$

The initial offset and pitch angles are small and, using the small angle approximations $\cos\alpha \approx 1$ and $\sin\alpha \approx \alpha$:

$$\ddot{z}_M = \ddot{z} - \ddot{x}\theta - \ddot{x}\delta$$

If it is further assumed that the pitch angle of the vehicle relative to the pavement surface is a linear function of longitudinal acceleration relative to the pavement surface, then:

$$\delta = C\,\ddot{x}, \text{ and } \ddot{x}\delta = C\,\ddot{x}^2$$

where C is a constant of proportionality with units of radians/m/s^2.

Including an offset for gravity and drift in the instrumentation electronics, , the measured acceleration is given by: $\ddot{z}_0$

$$\ddot{z}_M = \ddot{z}_0 + \ddot{z} - \ddot{x}\theta - C\,\ddot{x}^2$$

and, rearranging the equation, an approximation of the true vertical acceleration is:

$$\ddot{z} = \ddot{z}_M - \ddot{z}_0 + \ddot{x}\theta + C\,\ddot{x}^2$$

Note that the term associated with initial pitch angle, θ, changes sign with , whereas the term associated with pitch change always has the same sign. Vertical velocity is now found by integration: $\ddot{x}$

$$\begin{aligned}\dot{z} &= \dot{z}_0 - \int \ddot{z}_0 .dt + \int \ddot{z}_M .dt + \theta \int \ddot{x}.dt + C\int \ddot{x}^2 .dt \\ &= \dot{z}_0 - \ddot{z}_0\, t + \dot{z}_M + \dot{x}\theta + \dot{z}_S C\end{aligned}$$

where = vertical velocity at $t = 0$ and . $\dot{z}_0 \dot{z}_S = \int \ddot{x}^2 .dt$

All quantities are sampled at time increments of Δ seconds and all data processing is done digitally. Therefore, the equation for vertical velocity can be rewritten in terms of the sample index, i, and numerically integrated quantities, with the first sample numbered 0:

$$\dot{z}_i = \dot{z}_0 - i\Delta.\ddot{z}_0 + \dot{z}_{Mi} + \dot{x}_i\,\theta + \dot{z}_{Si} C$$

Adjusting , , θ, and C so that is minimized over the full length of a digitized profile record proved to be a reasonable strategy for removing the majority of the errors due to acceleration coupling as well as for stabilizing the integration process. Therefore, following the normal procedure for computing least squares coefficients (Press, 1992) gives: $\dot{z}_0 \ddot{z}_0 \dot{z}^2$

$$\sum \dot{z}_i^2 = \sum \left(\dot{z}_0 - i\Delta.\ddot{z}_0 + \dot{z}_{Mi} + \dot{x}_i\,\theta + \dot{z}_{Si} C\right)^2 = \text{minimum}$$

Differentiating with respect to , , θ, and C in turn and equating the resulting expressions to zero gives the following matrix equation (where N = the total number of samples): $\dot{z}_0 \ddot{z}_0$

$$\begin{pmatrix} N & -\Delta\sum i & \sum \dot{x}_i & \sum \dot{z}_{Si} \\ -\Delta\sum i & \Delta^2\sum i^2 & -\Delta\sum i\dot{x}_i & -\Delta\sum i\dot{z}_{Si} \\ \sum \dot{x}_i & -\Delta\sum i\dot{x}_i & \sum \dot{x}_i^2 & \sum \dot{x}_i\dot{z}_{Si} \\ \sum \dot{z}_{Si} & -\Delta\sum i\dot{z}_{Si} & \sum \dot{x}_i\dot{z}_{Si} & \sum \dot{z}_{Si}^2 \end{pmatrix} \begin{pmatrix} \dot{z}_0 \\ \ddot{z}_0 \\ \theta \\ C \end{pmatrix} = \begin{pmatrix} -\sum \dot{z}_{Mi} \\ \Delta\sum i\dot{z}_{Mi} \\ -\sum \dot{x}_i\dot{z}_{Mi} \\ -\sum \dot{z}_{Si}\dot{z}_{Mi} \end{pmatrix}$$

The matrix equation is solved after all of the summations have been computed over the full record length. The procedure is only applicable for a record of reasonable length. (Other similar but more complicated procedures are available for real-time processing of such signals. But they would probably not be suitable for the present application because of the comparatively short records and the rapid changes in conditions (Stengel, 1994, and Press, 1992).) Integrating the corrected vertical velocity, , adding the displacement sensor signal, and applying a linear correction to give the start and end points the same value (usually zero) completes the computation of the elevation profile with respect to time. The profile is converted to a spatial record by low-pass filtering and then eliminating all data points except for those occurring closest to each tenth traveled distance pulse. Final sample spacing is therefore 25 mm (1 in). A scheme in which the elevation sample values are averaged between distance pulses is used when the vehicle speed falls below the point where serious aliasing of the decimated signal would occur. $\dot{z}$

As an example of the effects of the processing, figures 2 through 9 below show results for a profile measurement made 3 m (10 ft) to the right of the center line of Runway R1 before the runway was overlaid. The normal test procedure is to align the test vehicle at the runway threshold, accelerate to the test speed, travel the majority of the length of the runway under cruise control, and brake to a full stop at the opposite threshold. But in this case a construction truck crossed the runway during the measurement and the driver of the test vehicle was forced to brake and then accelerate back to the test speed. With no compensation applied to the accelerometer signal, except to force the end-points of the velocity and position signals through zero, extreme errors are apparent during the periods when the vehicle is accelerating or braking. Also note the asymmetry of the errors in the velocity signal caused by the combination of linear and squared terms in the error equation, mentioned above.

The calculated total vertical motion of the vehicle is 6.2 m (20.4 ft) compared to the corresponding distance measured by a rod and level survey of 0.6 m (1.9 ft) (see figure 9). But after applying the compensation scheme, the vertical velocity signal has a much smaller range and the rapid changes associated with the acceleration and braking of the test vehicle have been reduced to the extent that they cannot be visually distinguished from the rest of the signal except, perhaps, at the very end of the record. Calculated total vertical motion has been reduced to 0.3 m (1 ft). This is less than was measured in the rod and level survey; an effect caused by minimizing vertical velocity squared about the straight line connecting the ends of the profile. Curves fit through a few coarsely spaced points along the pavement can be used as the minimization datum to generate detailed profiles much closer to the true absolute profile.

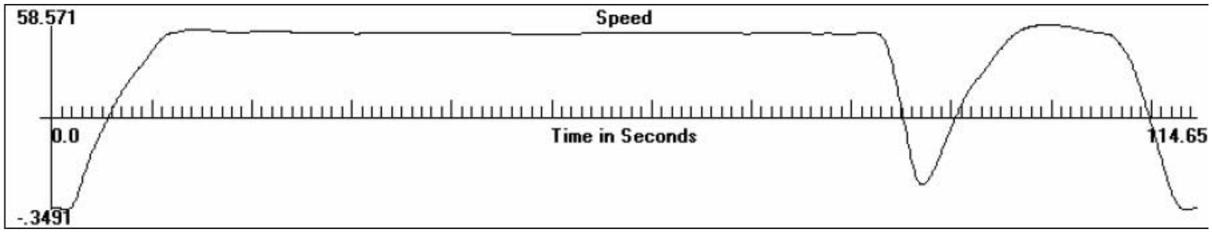

Figure 2. Test vehicle speed, ft/s, total record length = 114.65 seconds.

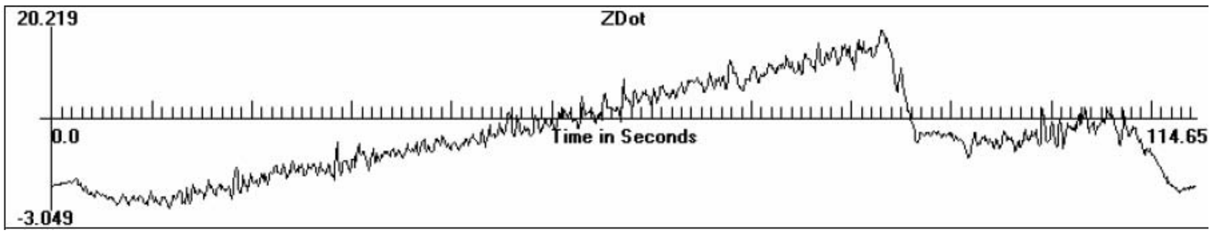

Figure 3. Vertical velocity of the test vehicle at the accelerometer, no compensation, in/s.

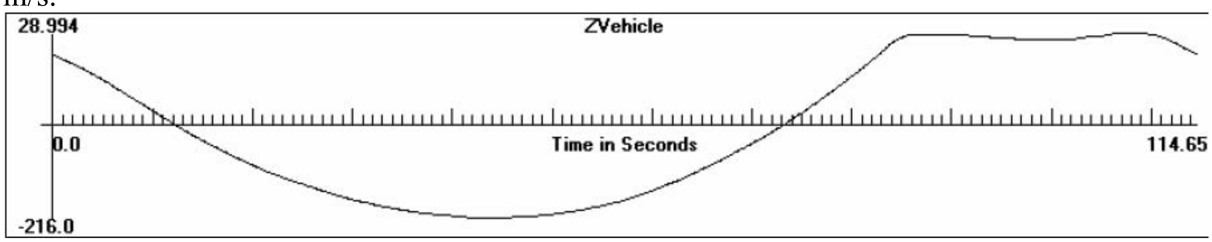

Figure 4. Vertical (inertial) position of the test vehicle at the accelerometer, no compensation, in.

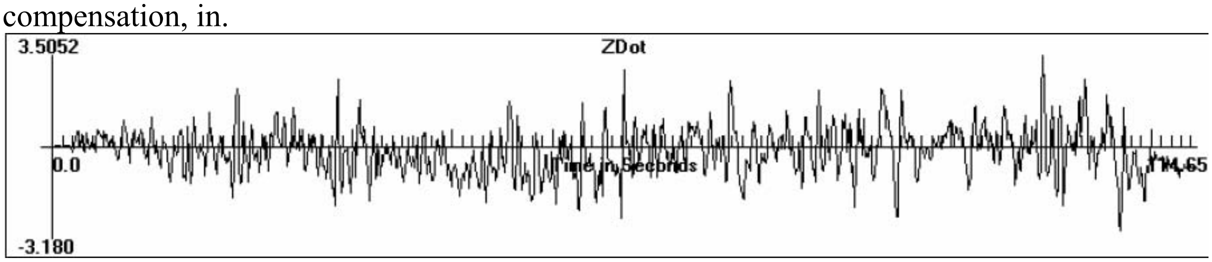

Figure 5. Vertical velocity of the test vehicle at the accelerometer, full compensation, in/s.

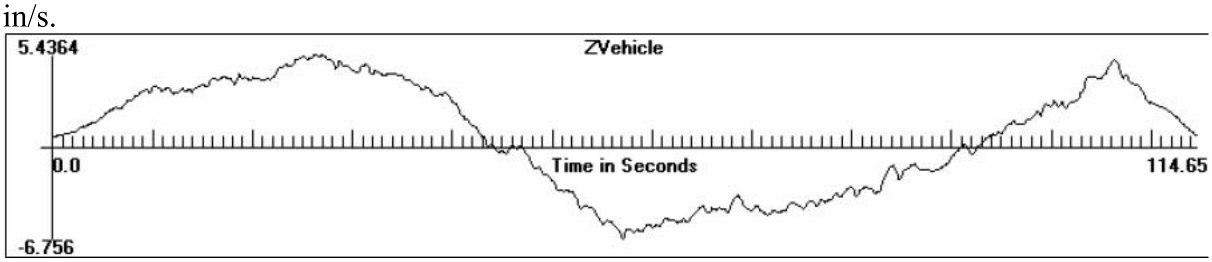

Figure 6. Vertical (inertial) position of the test vehicle at the accelerometer, full compensation, in.

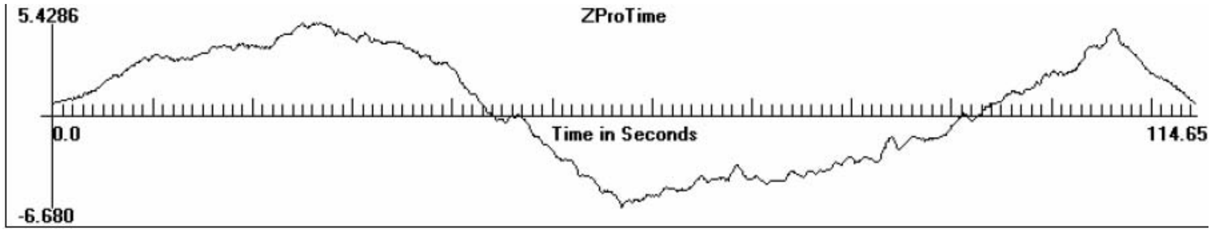

Figure 7. Elevation profile with respect to time, full compensation, in.

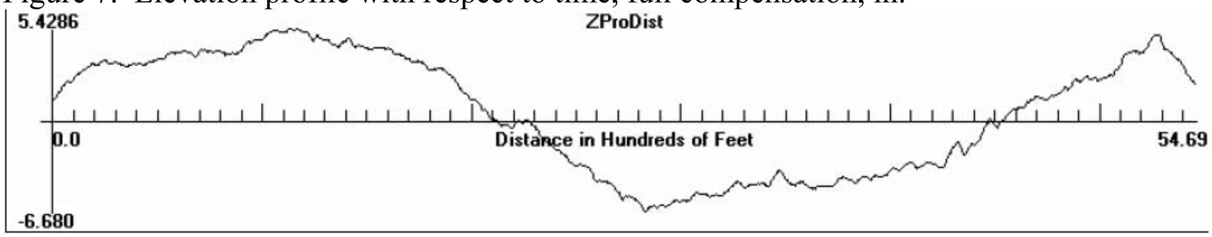

Figure 8. Elevation profile with respect to distance, full compensation, in. Total length = 1,667 m (5,469 ft).

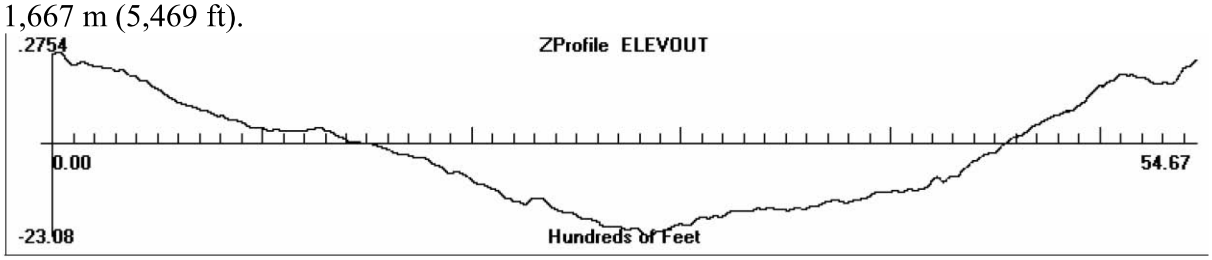

Figure 9. Rod and level survey, in, at 7.62 m (25 ft) spacing along the centerline of the runway.

BEFORE AND AFTER ON RUNWAY R1

Profiles were also measured on Runway R1 after the overlay had been placed. Figures 10 and 11 show the deviations from a simulated 3.6-m (12-ft) straightedge computed for profiles measured 3 m (10 ft) from the centerline of the runway. The deviations were computed once every 25 mm (1 in) along the profile. The difference in the record lengths was caused by construction signs which were erected prior to overlaying of the pavement and which obstructed the ends of the runway. Probability distribution functions were also computed (figure 12) and the 85th percentile deviations (85%) determined. By these measures, the pavement on that profile line became rougher as a result of the overlaying operation. However, with one exception on the overlaid pavement, the measurements are well within FAA advisory standards. The exception is a computed deviation from the straightedge of approximately 17 mm (0.65 in). A zoomed view of the profile, with the straightedge and deviation

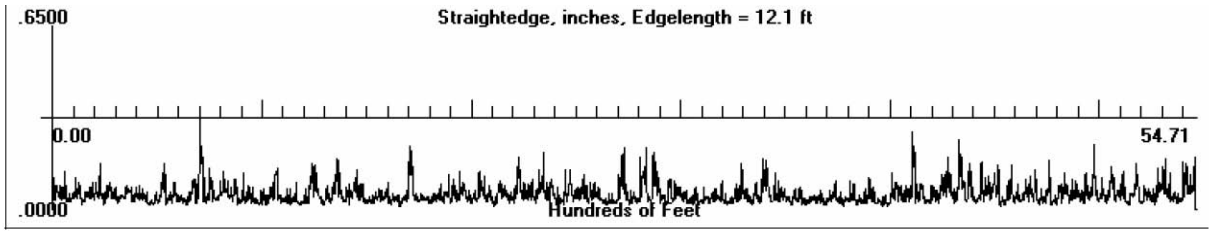

Figure 10. Straightedge before overlay, average = 1.4 mm (0.05 in), 85% = 2.1 mm (0.083 in).

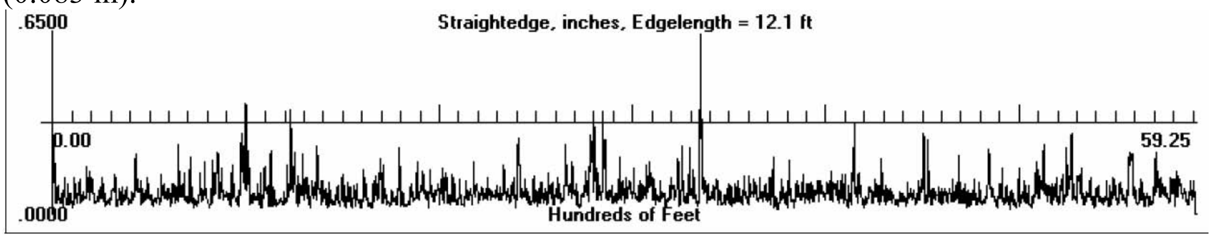

Figure 11. Straightedge after overlay, average = 1.9 mm (0.075 in), 85% = 2.7 mm (0.11 in).

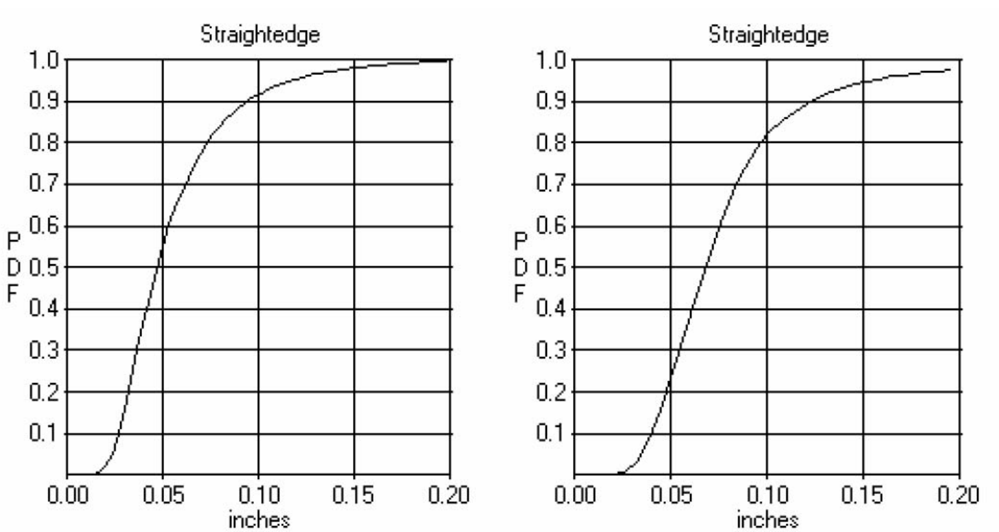

Figure 12. Probability distribution functions for the straightedge deviations. Before overlay is on the left and after overlay is on the right.

line included, is shown in figure 13. The cause of the large deviation is a change in elevation height of 14 mm (0.55 in) over a distance of 1.4 m (4.75 ft). (The extreme deviation occurs with the straightedge further to the left, but the position in the figure shows the problem area more clearly.) Visual inspection of the pavement showed that the disturbance was caused by a poorly formed transverse joint extending across about one quarter the width of the runway. Figures 14 and 15 show computed displacements of the measuring wheel of a simulated 12-wheel California Profilograph for the same profiles. A +/- 2.54 mm (0.1 in) blanking band is also shown. The results are very similar to those for the straightedge except that the relative magnitudes of the pavement disturbances are, in some cases, quite different. (see ACPA, 1990, for the definition of PI). The large indicated disturbance toward the left end of the runway is due to a drop in the pavement of 28 mm (1.1 in) over approximately 6 m (20 ft) followed by a shallower rise. These distances along the pavement are longer than the straightedge length but about the same order as the length of the profilograph. The disturbance would therefore not be expected to be as prominent on the straightedge record.

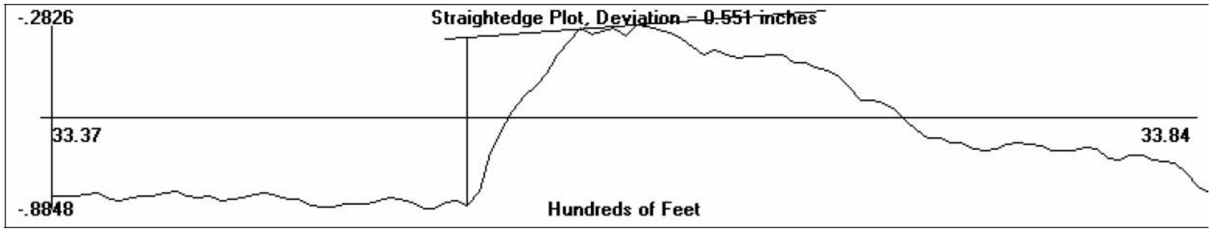

Figure 13. Zoomed profile corresponding to figure 11 and with straightedge included.

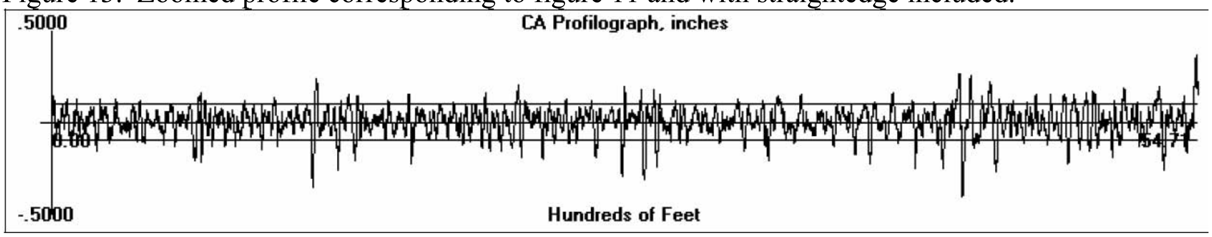

Figure 14. Profilograph before overlay, PI = 2.3 in/mile.

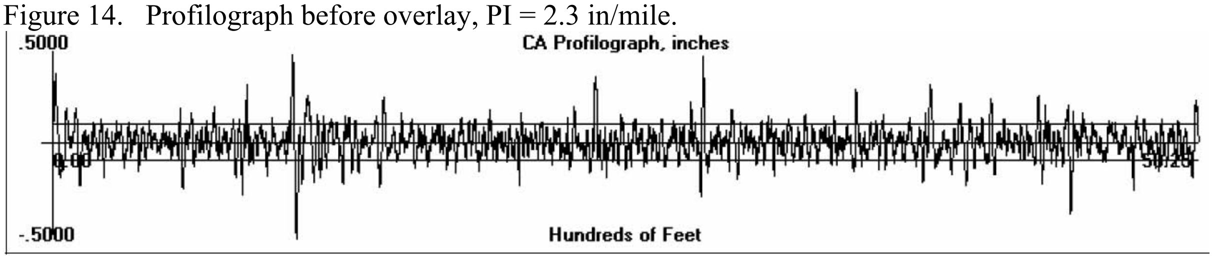

Figure 15. Profilograph after overlay, PI = 4.7 in/mile.

AFTER OVERLAYING ON R2

Profile measurements were also made on Runway R2 before and after overlaying. However, except to say that roughness increased somewhat on this runway as well, only the roughness of the pavement measured after overlaying will be discussed. Figure 16 shows a profile measured approximately 1 m (3 ft) to the side of the centerline. Figures 17 and 18 show straightedge and profilograph plots respectively. The runway is much rougher than Runway R1 except at the ends, which were completely closed when that part of the runway was overlaid. The 85th percentile straightedge deviation, at 5.3 mm (0.21 in), is close to the FAA advisory maximum. Over smaller sections, the limit may be exceeded, although it should be said that the procedure for computing the 85th percentile is quite different than the manual method and a correlation between the two methods has not been made. The Boeing Bump criteria is shown in figure 19 for comparison with an index which tends to favor longer length disturbances (a pavement is rated unsatisfactory by the Boeing criteria when the bump index exceeds a value of 1). Very distinct disturbances are identifiable at the same positions on all of the plots. These disturbances are typically associated with transverse joints. Measurements were also made of the response of an instrumented B-727-100QC aircraft operated by the FAA William J. Hughes Technical Center. Figures 20 through 24 show the vertical accelerations and vertical strut loads for a run made with a maximum speed of 100 knots. The nose gear responses marked in figure 23 correspond with the pavement disturbances marked in figure 17. Maximum accelerations measured at the cg and the cockpit are both close to, or above, the generally accepted maximums for aircraft ride quality. However, the measurements were made at a sample rate of 240 Hz and were low-pass filtered with a cutoff frequency of 10 Hz. Changing the filter frequency will make a considerable difference to the magnitudes of the measured maximum accelerations. Specifications for limits on allowable maximum accelerations should include details on the intended bandwidth of the aircraft responses to be measured and on the signal processing requirements.

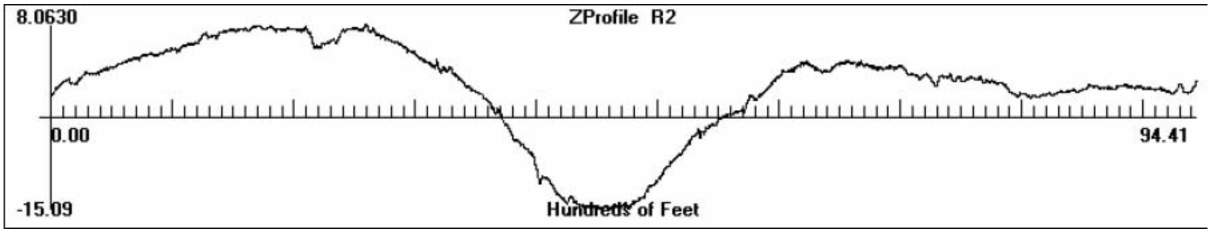

Figure 16. Profile on Runway R2 measured after overlaying.

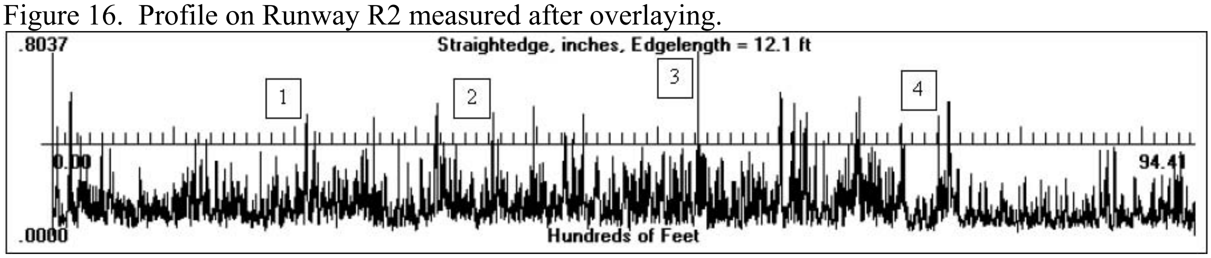

Figure 17. Straightedge on Runway R2, average = 3.5 mm (0.136 in), 85% = 5.3 mm (0.21 in).

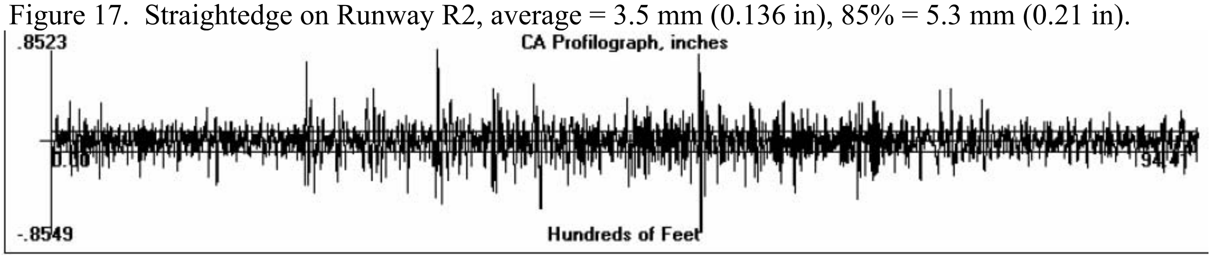

Figure 18. Profilograph on Runway R2. PI = 21.3 in/mile over the full length. For 300 m (1,000 ft) section lengths PI varies from 7 at the ends to 34 for the section containing the largest disturbance.

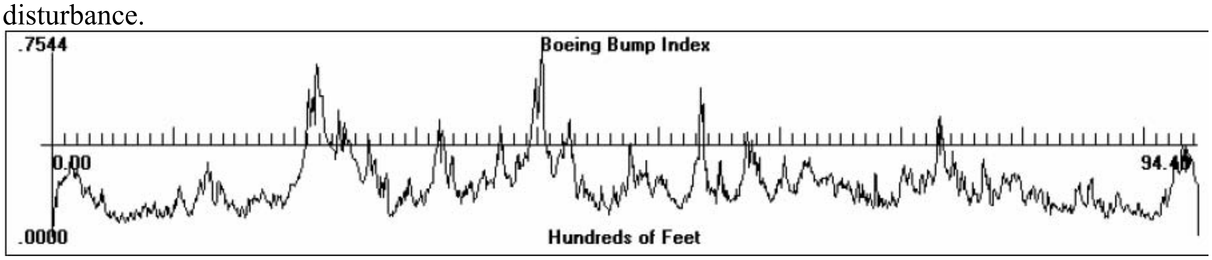

Figure 19. Boeing Bump Index on Runway R2.

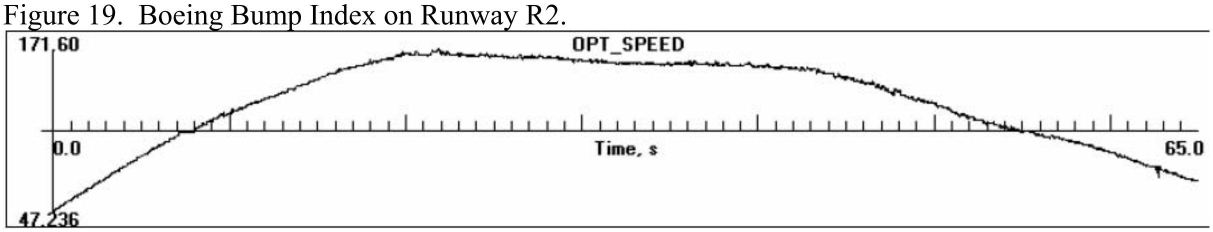

Figure 20. B-727 aircraft speed, ft/s (1 ft/s = 0.3048 m/s). Target speed was 100 knots (168 ft/s).

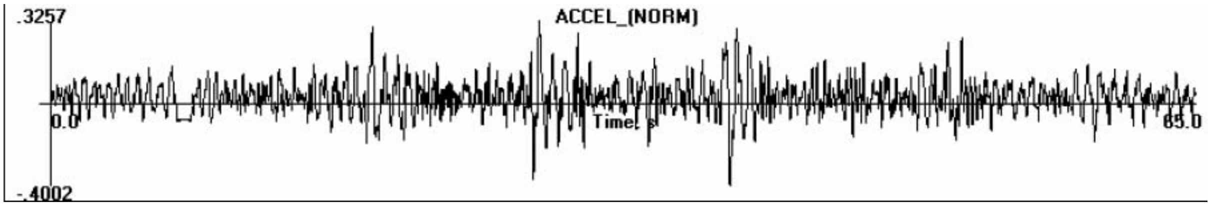

Figure 21. B-727 aircraft: vertical acceleration at the center of gravity (g), on the cabin floor.

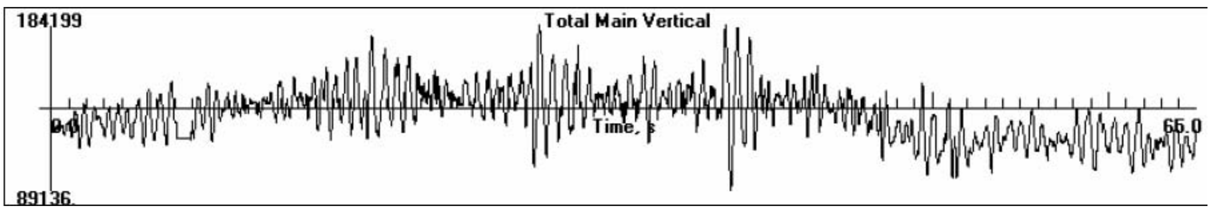

Figure 22. B-727 aircraft: sum of left and right main gear strut vertical loads.

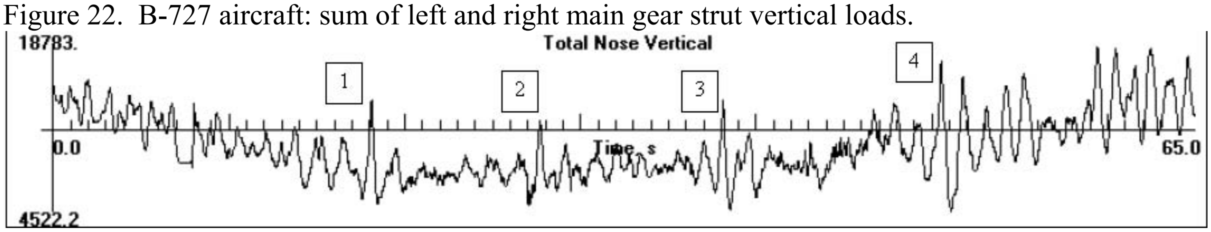

Figure 23. B-727 aircraft: nose gear strut vertical loads.

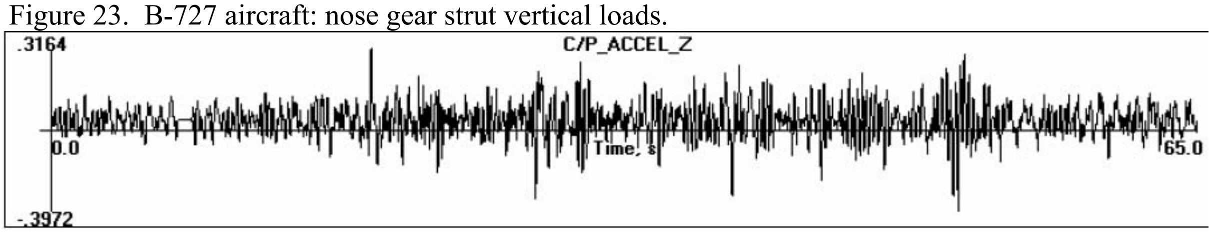

Figure 24. B-727 aircraft: vertical acceleration at the cockpit floor.

CONCLUSIONS

Suitable procedures and equipment have been developed for rapidly measuring airport pavement elevation profiles and computing roughness indices from the measured profiles. The index variables (deviation from a straightedge, for example), when plotted over the full length of a runway or taxiway, provide a convenient means of identifying possible rough areas and evaluating strategies for remediation.

Overlaying airport pavements during nightly closures can result in rougher pavements than would normally be expected because of the large number of lateral construction joints necessitated by this type of schedule. Measurements were made on two asphalt overlay projects, with a significant difference being shown between the roughness of the resulting pavements.

Construction practices used during the nightly startup and close-down phases clearly play an important role in the quality of the pavement surfaces. However, other differences between the two projects, both structurally and procedurally, may play equally significant roles and more evaluation is required before drawing further conclusions. It should also be noted that the projects were selected for evaluation before rehabilitation began.

ACKNOWLEDGEMENTS

The work described in this paper was conducted under FAA contract No. DTFA03-93-C-00021, William J. Hughes Technical Center, Atlantic City, NJ, USA, COTR Satish K. Agrawal.

REFERENCES

Pong, Meau-Fu and Wambold, J.C., "Evaluation of Accelerometer Established Inertial Profiling Reference Computation Methods," 71st Annual Meeting of the TRB, Washington, DC, USA, 1991.

Stengel, R.F., "Optimal Control and Estimation," Dover Publications, Mineola, NY, USA, 1994.

Press, H.P., Teukolsky, S.A., Vetterling, W.T. and Flannery, B.P., "Numerical Recipes in FORTRAN," Cambridge University Press, 1992.

ACPA, "Constructing Smooth Concrete Pavements," Technical Bulletin TB-006.0-C, 1990.

DeBord, K.J., "Runway Roughness Measurement, Quantification, and Application - the Boeing Method," Boeing Document No. D6-81746, Boeing Commercial Airplane Company, USA, 1990.